Estimation Of Gps Receiver Dcb's By Using Gagan Observations

K.Siva krishna, P. Sai Keerthi, T. D. L. N. Prathyusha, M. Bhanu Prakash Reddy, D.V.Ratnam

Abstract: Many errors impair the precise positioning of the GPS, the ionospheric lag being the most prevalent error. The line-of-sight TEC derived from GPS dual frequency information is skewed by GPS satellite and receiver DCB's. There are DCB's as the two frequencies of the GPS experience various delays in the GPS satellite and receiver hardware. The recipient instrumental bias estimate plays an important role in achieving the precise navigation required for civil aircraft users. In this paper, we have estimated the ionospheric delay without removing the DCB's and then separated the DCB's from the resultant output to obtain required ionospheric delay in a station.

Index Terms: GAGAN, GPS, TEC, SBAS, Ionospheric Delay, Pseudo Range, DCB's.

1.INTRODUCTION

Global Positioning System (GPS) is currently widely used for navigation and positioning in either kinematic or static mode in a number of applications. Ionospheric interference can reduce tens of meters of positioning accuracy. The ionospheric impact could reach more than a hundred meters during a violent ionospheric storm. After being switched off for single-frequency users since Selective Availability (SA) [2], this ionospheric effect appears to have become the largest source of error in GNSS navigation and positioning. The ionospheric effects therefore need to be considered for high precision positioning. The ionosphere's TEC can be easily estimated from the GPS data combination. GPS measurements-based TEC data are uncertain because every GPS bias that seriously affects the accuracy of the ionospheric TEC estimates [1],[6]. satellite transmitter and receiver hardware have associated A useful tool for calculating the ionospheric TEC is the GPS. A GPS satellite transmits dual-frequency signals to enable ionospheric delays to be extracted. However, the measured differential delays include not only the delay caused by the ionospheric TEC, but also the delay generated by the GPS satellite transmitters and ground receivers ' internal electronic circuits. The latter delay is known as instrumental bias (or bias in the inter frequency). Therefore, we need to remove these instrumental prejudices for the purpose of accurate measurement of TEC. Many approaches for evaluating receiver biases have been suggested.

1.1. DCB

DCB's are the errors which are obtained from variations observed in GNSS codes that are measured at same or different frequencies [1]. These DCB's are mainly used to extract TEC of ionosphere and to find the code-based position of GNSS receiver. Regional GPS network is an approach for the estimation of DCB receiver. To prevent singularities in the estimation of constraints, DCB's can set an arbitrary reference value. DCBs are primarily of two forms, namely inter-frequency bias, can be obtained by subtracting results at two dissimilar frequencies and intra-frequency bias, can be obtained by subtracting observations at two similar frequencies in the same way. [1]. Generally, the DCB results are affected by space weather so we are calculating the DCB once in a day. The regular variability in DCBs is therefore relatively stable.

1.2. GAGAN

A few nations have implemented their own Augmentation System based on satellites. EGNOS, for example, covers most of the European Union (EU) in Europe, along with some neighbouring nations and regions. Other SBASs at national level include: United States : Wide Area Augmentation System(WAAS), Japan: Multi-utilitarian Satellite Augmentation System (MSAS) , China: Satellite Navigation Augmentation System (SNAS) (being developed), South Korea: Wide Area Differential Global Positioning System (WADGPS) (being developed), Russia: System for Differential Corrections and Monitoring (SDCM) (being developed), India: GPS and GEO Augmented Navigation (GAGAN)

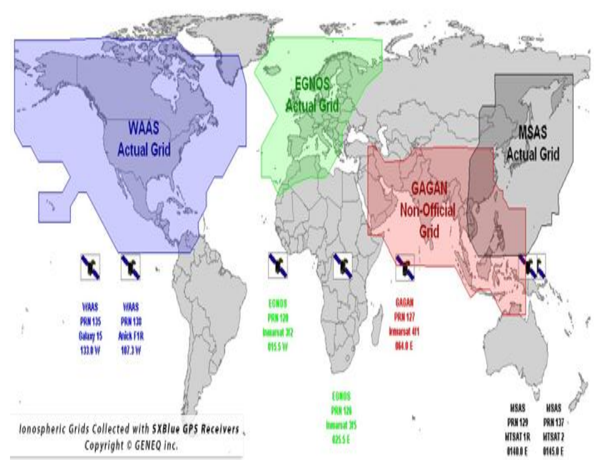

Indian Space Research Organization (ISRO) as well as Airports Authority of India (AAI) has implemented GAGAN project as Satellite Based Augmentation System for the safety of civil applications in Indian region. Not only for civil aviation the GAGAN system can be used by many users like public vehicles, shipping, etc. GAGAN is used to provide the correctness and availability of a data in a system. So, this data is more useful in airline operations to increase the air safety and the workload of air crew will be reduced [2]. For successful implementation, the GAGAN system consists of the following elements likely the Indian Reference Station (INRES) — across India 2 at 15 locations, Indian Master Control Centre (INMCC) — Bangalore 3's two, Indian Land Uplink Station (INLUS) — three stations, two Bangalore stations and one New Delhi station, Geostationary satellites

(GSAT8/GSAT10) in space and GSAT-15 on earth. A group of TEC stations are placed at different geographical areas all over India. At present there are 20 TEC stations in India and the resource are planning to increase it to 27 stations by placing them in the mid region of India since there is high variations in ionosphere. The received data from various stations is collected and sent to INMCC to assess the validity of signals and then resultant data is packed as GAGAN message and is transmitted to INLUS, which is situated at Bangalore [2]. The distribution of the 26 reference GPS continues mentoring stations used to develop the regional TEC model

No.	GAGAN- Station Name	Geographic latitude (deg.)	Geographic longitude (deg.)
1	Trivandrum	8.47	76.91
2	Madurai	9.83	78.09
3	Agartti	10.83	72.17
4	Port Blair	11.67	92.72
5	Banglore	12.95	77.68
6	Hubli	15.36	75.08
7	Hyderabad	17.44	78.47
8	Visakhapatnam	17.72	83.22
9	Mumbai	19.09	72.85
10	Aurangabad	19.86	75.39
11	Bhubaneswar	20.25	85.8
12	Nagpur	21.08	79.06
13	Raipur	21.18	81.73
14	Kolkata	22.64	88.44
15	Ahmedabad	23.06	72.61
16	Bhopal	23.28	77.34
17	Aizawl	23.83	92.62
18	Gaya	24.74	84.94
19	Khajuraho	24.82	79.92
20	Gauhati	26.12	91.59
21	Jodhpur	26.26	73.05
22	Bagdogra	26.68	88.32
23	Lucknow	26.76	80.88
24	Agra	27.16	77.97
25	Delhi	28.58	77.21
26	Shimla	31.08	77.06

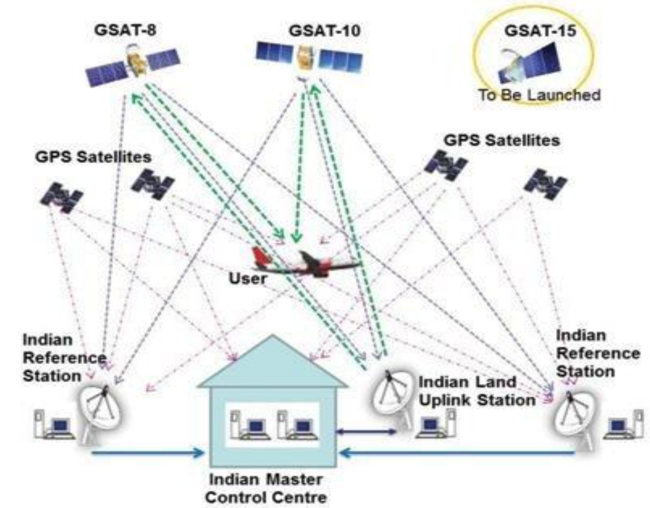

1.3. TEC

The total Electron Content (TEC) is the total count of electrons in the direction between a radio transmitter and the receiver. The interaction of electrons affect radio waves. The more electrons in the radio wave's way, the greater effect on the radio sign. TEC is a good testing criterion for potential spatial impact for earth-to-satellite correspondence and satellite path. TEC is measured in electrons per square meter. TECU= 10 ^ 16 TEC unit electrons / m2. Vertical TEC esteems in the ionosphere of Earth can range from a few to a few hundred TECUs. The ionosphere-based TEC is changed by adjusting Extreme Ultra-Violet radiation dependent on sunlight, geomagnetic disturbances, and barometric waves spreading from the lower atmosphere. Therefore, the TEC must depend on nearby time, distance, longitude, season, geomagnetic conditions, cycle and movement based on the sun, and conditions in the troposphere. The ionosphere affects the release of radio waves. The speed of the radio waves varies as the sign in the ionosphere passes through the electrons. An ionosphere-proliferating electromagnetic wave's all-out postponement depends on both the recurrence of the radio wave and the TEC between the transmitter and the receiver. At certain wavelengths, the ionosphere is penetrated by radio waves. The ionosphere for different frequencies reflects the waves. The adjustment in the ionosphere's way and speed of radio waves greatly affects the accuracy of satellite route frameworks, such as GPS/GNSS. Changes in the TEC ionosphere will result in several meters of error in the position figures [3].

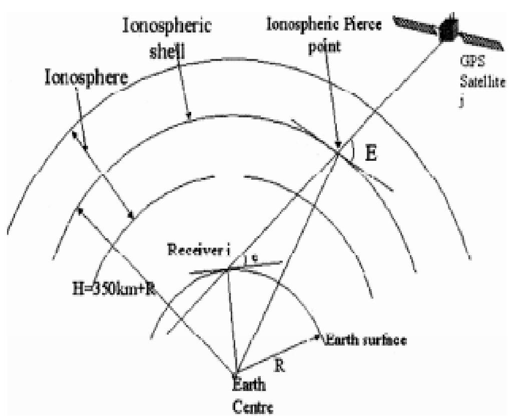

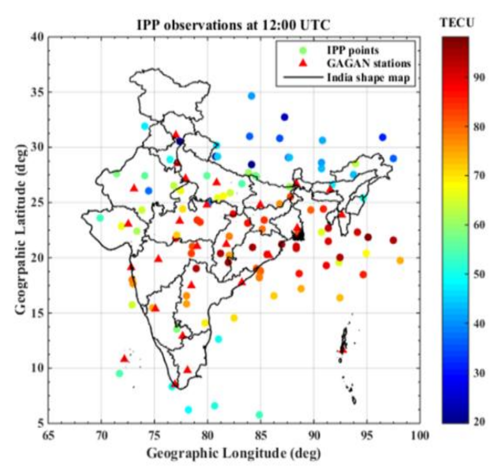

2. METHODOLOGY

$$P^{i}_{k,j} = \rho^{i}_{j} + d^{i}_{ion,k,j} + d^{i}_{trop,j} + c(\tau^{i} - \tau_{j}) + d^{i}_{k} + d_{k,j} + \varepsilon^{i}_{p,k,j} \quad (1)$$

$$L^{i}_{k,j} = \rho^{i}_{j} - d^{i}_{ion,k,j} + d^{i}_{trop,j} + c(\tau^{i} - \tau_{j})$$

$-\lambda\left(b_{k,j}^{i} + N_{k,j}^{i}\right) + \varepsilon_{k,j}^{i}$ (2)

If P represents the measurement of pseudo-range GPS, L is the measurement of phase of the GPS operator, q is the actual distance between the GPS receiver (j) and satellite(i), d_{ion} represents the delay of ionosphere, d_{trop} represents the delay of troposphere, c represents light rate in vacuum, τ^{i} is clock error of satellite, τ_j is the receiver clock error of the receiver, the remaining d are the code delays for the satellite and receiver instrument biases b is the progression of satellite and receiver biases, N is the carrier phase ambiguity, and ε are the GPS measurement residuals. Here, the subscript (k = 1, 2) this is the frequency, the superscript I is the GPS satellite's PRN, and the subscript j is the GPS receiver [1]. The ionosphere lag is determined by using the dual-frequency measurements as, let us suppose $f_{L1} = 1575.4$ MHz and $f_{L2} = 1227.6MHz$ then

$$P_4 = P_{1,j}^{i} - P_{2,j}^{i} = \left(d_{ion,1,j}^{i} - d_{ion,2,j}^{i}\right) + DCB^{i} + DCB_j \quad (3)$$

$$L_4 = L_{1,j}^{i} - L_{2,j}^{i} = -\left(d_{ion,1,j}^{i} - d_{ion,2,j}^{i}\right) - \lambda\left(b_{1,j}^{i} - b_{2,j}^{i}\right) - \lambda\left(N_{1,j}^{i} - N_{2,j}^{i}\right) \quad (4)$$

here $DCB^{i} = L_{1,j}^{i} - L_{1,j}^{i}$ and

$$DCB_j = d_{1,j} - d_{2,j}$$

are the satellite and receiver differential code biases. Due to the presence of larger noise in the pseudo range P_4, we use carrier phases to smooth the pseudorange. Now the smoothed observation is done by the equation

$$P_{4,sm} = \omega_t P_4(t) + (1 - \omega_t)P_{4,prd}(t) \quad (5)$$

t is the number of epoch and (t > 1), ω_t is weight factor of that is related to t and

$$P_{4,prd}(t) = P_{4,sm}(t-1) + [L_4(t) - L_4(t-1)] \quad (6)$$

If the value of t=1 it indicates the first arc epoch $P_{4,prd}$ is same as P_4 after smoothing it. The ionospheric delay is expressed as

$$d_{ion} = \frac{40.3}{f^2} STEC \quad (7)$$

here f represents the carrier frequency and STEC represents the Slant TEC of signal. Now replace d_{ion} value in $P_{4,sm}$ then

$$P_{4,sm} = 40.3\left(\frac{1}{{f_1}^2} - \frac{1}{{f_2}^2}\right) STEC + DCB^{i} + DCB_j \quad (8)$$

Now from the above equation we can express STEC equation as follows:

$$STEC = \frac{f_1^2 f_2^2}{40.3(f_1^2 - f_2^2)}\left(P_{4,sm} - cDCB_j - cDCB^{i}\right) \quad (9)$$

$$DCB_j = P_{4,sm} - DCB^{i} \quad (10)$$

Receiver DCBj values is estimated from the Eq.(10)

3.Results and Discussion

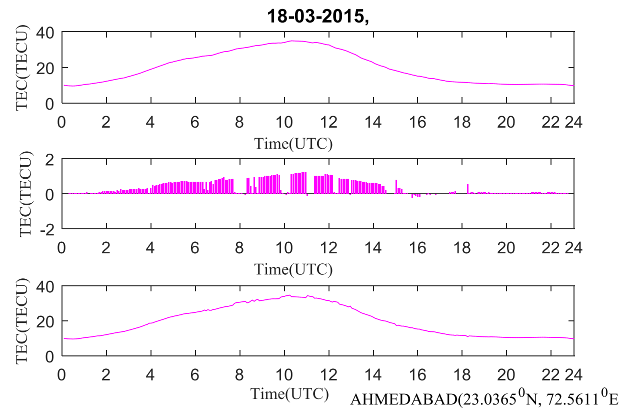

(a) Plot 1

Station Name: Ahmedabad (23.0365° N, 72.5611° E)

In Fig1 we observed the plot of Ionosphere Delay without removing DCB's where Time is represented on X-axis and TECU is represented on Y-axis. In Fig2 we plotted a graph of DCB's on 18th March 2015. It is observed that DCB's are high from 10 am to 12pm, approximately equal to 1.6 TECU and very low at night-time approximately equal to zero. In Fig3 by removing the DCB's from Fig1 we are plotting the Ionospheric delay.

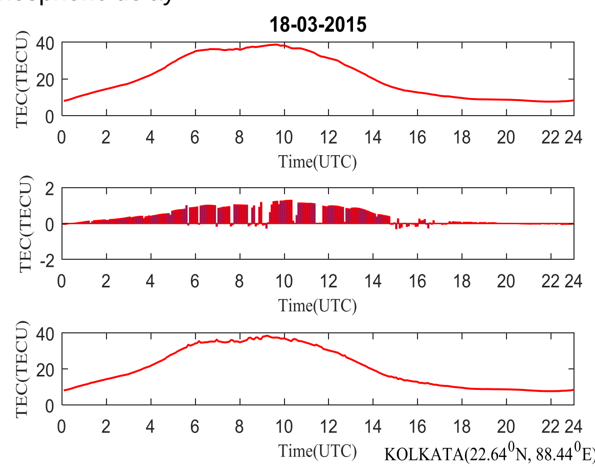

(b) Plot 2

Station Name: Kolkata (22.64°N, 88.44° E)

In Fig1 we observed the plot of Ionosphere Delay without removing DCB's where Time is represented on X-axis and TECU is represented on Y-axis. In Fig2 we plotted a graph of DCB's on 18th March 2015. It is observed that DCB's are high from 6 am to 2pm, approximately equal to 1.8 TECU and very low at night time approximately equal to zero. In Fig3 by removing the DCB's from Fig1 we are plotting the Ionospheric delay.

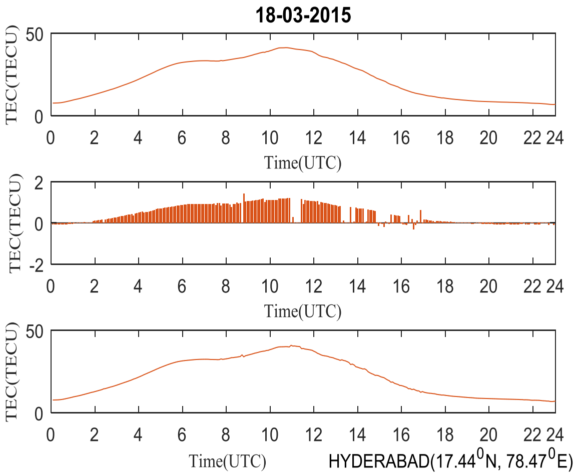

(c) Plot 3

Station Name: Hyderabad (17.44° N, 78.47° E)

In Fig1 we observed the plot of Ionosphere Delay without removing DCB's where Time is represented on X-axis and TECU is represented on Y-axis. In Fig2 we plotted a graph of DCB's on 18th March 2015. It is observed that DCB's are high from 5 am to 1pm, approximately equal to 1.7 TECU and very low at night-time equal to zero. In Fig3 by removing the DCB's from Fig1 we are plotting the Ionospheric delay.

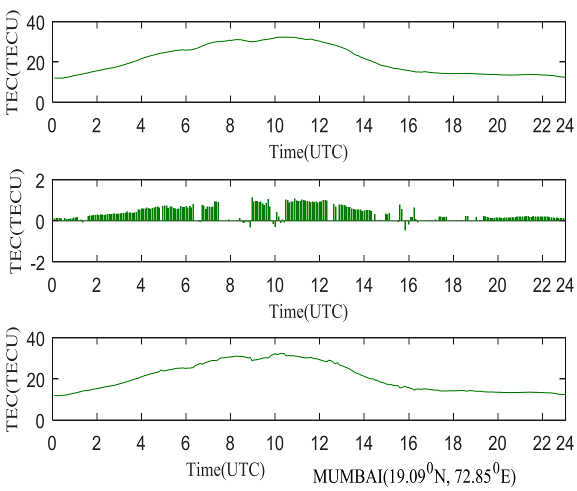

(d) Plot 4

Station Name: Mumbai (19.09°N, 72.85° E)

In Fig1 we observed the plot of Ionosphere Delay without removing DCB's where Time is represented on X-axis and TECU is represented on Y-axis. In Fig2 we plotted a graph of DCB's on 18th March 2015. It is observed that DCB's are high from 9am to 12pm, approximately equal to 1.5 TECU and very low at night-time approximately equal to zero. In Fig3 by removing the DCB's from Fig1 we are plotting the Ionospheric delay.

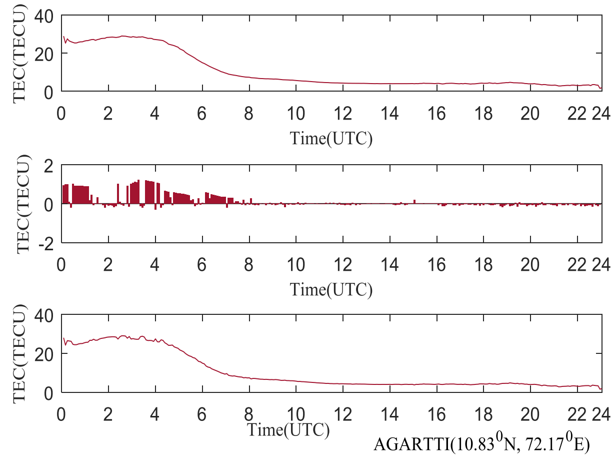

(e) Plot 5

Station Name: Agartti(10.83° N, 72.17° E)

In Fig1 we observed the plot of Ionosphere Delay without removing DCB's where Time is represented on X-axis and TECU is represented on Y-axis. In Fig2 we plotted a graph of DCB's on 18th March, 2015. It is observed that DCB's are high from 2 am to 4 am, approximately equal to 1.5 TECU and from 8 am it is equal to zero. In Fig3 by removing the DCB's from Fig1 we are plotting the Ionospheric delay.

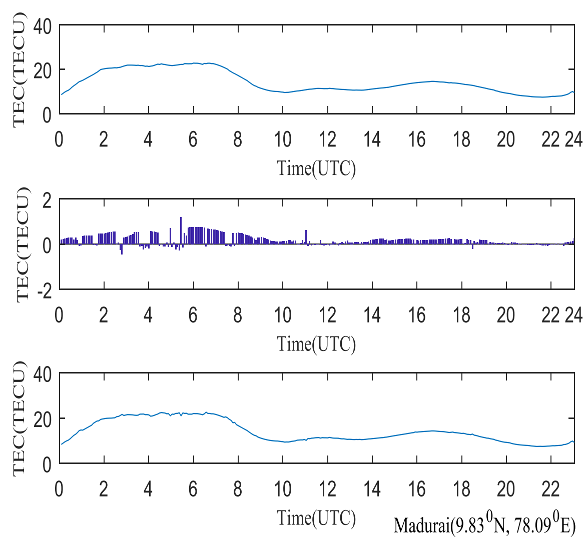

(f) Plot 6

Station Name: Madurai(9.83° N, 78.09° E)

In Fig1 we observed the plot of Ionosphere Delay without removing DCB's where Time is represented on X-axis and TECU is represented on Y-axis. In Fig2 we plotted a graph of DCB's on 18th March, 2015. It is observed that DCB's are high from 6 am to 8 am, approximately equal to 1.0 TECU and from 11 am it is approximately equal to zero. In Fig3 by removing the DCB's from Fig1 we are plotting the Ionospheric delay.

4. CONCLUSIONS

For the accurate position fixing of the user, error free estimation of TEC is required. So for the above reason we have estimated the ionospheric delay without removing the

DCB's and then separated the DCB's from the resultant output to obtain required ionospheric delay in a particular station. And from the above plots it is observed that DCB's are low at Agartti and Madurai stations when compared to other stations.

5. ACKNOWLEDGEMENT

The present work been carried out under the project titled 'Development of Single Frequency Ionospheric correction & plasma bubble detection algorithms using GPS Aided GEO Augmented Navigation (GAGAN) & Navigation Indian Constellation (NavIC) TEC observations' sponsored by NavIC– GAGAN Utilization Programme at Space Applications Centre, Ahmedabad, India, Project ID: NGP-10.

6. REFERENCES

[1] .Abid, Mohammed A., et al. "Temporary and spatial variability of differential biases: case study of Egyp t's regional network." Alexandria Technology Journ al 55.2 (2016): 1507-1514.
[2] .Rao, N.K. "Augmentation system based on the Ind ian satellite." 84.40. Ua (back in 2007).
[3] . Arikan F, Nayir H, Sezen U & Arikan O, GPS-TEC, Radio Sci (USA), 43 (2008) RS4004, doi: 10.1029/2007RS003785 Interfrequency Receiver Bias.
[4] . Using SVD algorithm, IEEE Trans Aerosp Electron Syst (USA), 44(4)(2008) pp 1560-1566, Sarma A D, Rao G S, Rao P V D S & Ramalingam K, GPS satellite and receiver biases.
[5] 5. Biel H A, A terrestrial station's geomagnetic time and place, J Atmos Terr Phys (UK), 52(9) (1990) pp 687-694.
[6] 6. Klobuchar J A, Ionospheric GPS single-frequency time-delay algorithm, IEEE Trans Aerosp Electron Syst (USA), 23(3)(1987) pp 325-331.
[7] 7. Wilson B D & Mannucci A, Instrumental biases in ionospheric measurements derived from GPS data, Proceedings of the Sixth International Satellite Division Meeting of the Navigation Institute, ION GPS-93 (Navigation Institute, Salt Lake City, Utah), 1993, pp 1343-1351.
[8] 8. Analysis of Seismo-Ionospheric Perturbations using Modified Covariance Algorithm SPIE Conference On Remote Sensing-April 2016 R.Revathi Dr.S.KoteswaraRao Proc. Of SPIE Vol.9877, 987730-1to 987730-7
[9] 9. Revathi, R., et al. "Application of maximum entropy method for earthquake signatures using GPSTEC." Multispectral, Hyperspectral, and Ultraspectral Remote Sensing Technology, Techniques and Applications VI. Vol. 9880. International Society for Optics and Photonics, 2016.
[10] 10. Revathi, R., et al. "Observation of ionospheric disturbances for earthquakes (M> 4) occurred during June 2013 to July 2014 in Indonesia using wavelets." Remote Sensing of the Atmosphere, Clouds, and Precipitation VI. Vol. 9876. International Society for Optics and Photonics, 2016.
[11] 11. Kiran, K. Uday, et al. "Identification of Coseismic Signatures by Comparing Welch and Burg Methods Using GPS TEC." Information and Decision Sciences. Springer, Singapore, 2018. 335-344.
[12] 12. Revathi, R., et al. "Instantaneous Time Smoothing in GPS Receivers Using Kalman Filter." Information and Decision Sciences. Springer, Singapore, 2018. 289-296.
[13] 13. Revathi, R., et al. "Application of Least Squares Algorithm for Precise GPS Receiver Positioning." Information and Decision Sciences. Springer, Singapore, 2018. 297-303.
[14] 14. Revathi, R., et al. "Application of Parametric Methods for Earthquake Precursors Using GPS TEC." Information and Decision Sciences. Springer, Singapore, 2018. 305-314.
[15] 15. Speech enhancement using discrete Kalman filter algorithm International Journal of Engineering and Technology (UAE) J. Shanmukha, Dr. K. S. Ramesh, Dr. S. Koteswara Rao Vol.7, No.2.7, pp.249-252, March 2018.
[16] 16. Application of klauder wavelet for generation of synthetic seismic signal International Journal of Engineering and Technology (UAE) A.Saritha, A.Neelima, Dr. K. S. Ramesh, Dr. S. Koteswara Rao Vol.7, No.2.7, pp.903-905, March 2018
[17] 17. Application of zero phase wavelet with International Journal of Engineering and Technology (UAE) P on artificial seismic signals. Sireesha, G. Sai Srinivas, Dr. K. S. Ramesh, Dr. S. Koteswara Rao Vol.7, No.2.7, March 2018, pp.906-908.
[18] 18. Analysis of seismic signal using maximum entropy method International Journal of Innovative Technology and Exploring Engineering K. Himaja, K. S. Ramesh, S. Koteswara Rao Feb'19,Vol 8,Issue 4,pp247-251.
[19] 19. Kiran, Uday, S. Koteswara Rao, and K. S. Ramesh. "Implementation of ESPRIT Algorithm on GPS TEC for Percussive Signatures of Earthquakes in Ionosphere." International Journal of Control Theory and Applications, Vol. 10, No. 5, p. 133-138, 2017 10 (2017): 133-138.
[20] 20. Performance analysis of Bartlett and Welch Methods for Earthquake Signatures Using GPS TEC International Journal of Control Theory and Applications K.Uday, Dr. S.Koteswara Rao Volume 10, Issue 5, 2017, Pages 569-575
[21] 21. Revathi, R., et al. "Application of Parametric Methods for Earthquake Precursors Using GPS TEC." Information and Decision Sciences. Springer, Singapore, 2018. 305-314.